Available online at www.sciencedirect.com
ScienceDirect
International Journal of Fatigue 29 (2007) 1941–1949
International Journal of Fatigue
www.elsevier.com/locate/ijfatigue

Corrosion-fatigue behaviour of 7075-T651 aluminum alloy subjected to periodic overloads

R.M. Chlistovsky, P.J. Heffernan *, D.L. DuQuesnay

Department of Mechanical Engineering, Royal Military College of Canada, Kingston, Ont., Canada K7K 7B4

Received 31 August 2006; received in revised form 15 January 2007; accepted 16 January 2007
Available online 26 January 2007

Abstract

The corrosion-fatigue behaviour of 7075-T651 aluminum alloy subjected to periodic overloads was examined. This aluminum alloy is typically used in aerospace structural components such as the wing spars of aircraft. Axial fatigue specimens were subjected to a loading spectrum that consisted of a fully reversed periodic overload of near-yield magnitude followed by 200 smaller cycles at high *R*-ratio. The specimens were fatigue tested while they were fully immersed in an aerated and recirculated 3.5 wt% NaCl simulated sea-water solution.

The results for the corrosion-fatigue testing were compared to data obtained for the same overload spectrum applied in laboratory air. A damage analysis showed that the presence of the corrosive environment accelerated the damage accumulation rate to a greater extent than that observed in air, particularly at low stress ranges. This resulted in a reduction in the fatigue strength of the material when it was simultaneously subjected to overloads and a corrosive environment. It is believed that the reduced fatigue life was due primarily to corrosion pit formation and a combination of anodic dissolution at the crack tip and hydrogen embrittlement. For practical purposes, the endurance-limit of the material disappears under these conditions.

Keywords: Corrosion; Fatigue; Periodic; Overloads; Aluminum

1. Introduction

Until around the year 1970, fatigue life calculations for components in the transportation industry were designed with a "safe-life" philosophy, based upon the use of Miner's rule combined with a damage parameter and a fatigue–resistance curve for the material This fatigue–resistance curve (i.e., S–N curve) was usually determined in lab-air under constant amplitude loading and then modified empirically to account for the variable amplitude loading conditions that the material would see in-service. Other methods of developing these curves consisted of testing several prototypes of the component under a measured loading regime found in-service to develop a standard stress-life curve for the piece. The use of these methods may lead to non-conservative results when predicting component durability under variable amplitude loading. Inevitably, loads in-service vary immensely and may be quite different from the loading used to obtain the stress-life curve. In addition, damage caused by a given stress-strain cycle is dependent on the previous cycles found in the load history of the component.

The majority of structural components experience variable amplitude load histories. These load histories can also contain periodic overload cycles that approach the yield strength of the material. For example, hard landings, severe turbulence or harsh manoeuvres during flight would be seen as overloads in the loading history of a wing spar of an aircraft. These occurrences have a marked effect on the cycles following the overload, and damage accumulation rates can increase substantially and remain elevated for thousands of cycles following an overload [1–3]. Furthermore, cycles of low stress/strain ranges that would

* Corresponding author. Tel.: +1 613 541 6000; fax: +1 613 542 8612.
E-mail address: pat.heffernan@rmc.ca (P.J. Heffernan).

0142-1123/$ - see front matter © 2007 Elsevier Ltd. All rights reserved.
doi:10.1016/j.ijfatigue.2007.01.010

not normally cause damage (i.e., below the endurance-limit of the material) can cause damage in the component for several hundred cycles following an overload cycle [1–4].

This phenomenon has been the subject of many studies and several models have been developed to explain the effect of load history on the fatigue damage evolution in subsequent cycles, the most recognized being the theory of crack-closure. The foundation of this theory is that the cycles can only be damaging to the component while the crack itself is open. The crack opening stress is a variable that changes continually throughout the life of the component and can be described as the stress required to keep the crack in the material open at its tip. This theory defines the effective stress range as the difference between the maximum stress and the crack opening stress – this is the actual part of the cycle that causes damage to the component. In previous work by the authors and co-workers [2–4,12,13], it was determined that a compressive underload peak immediately followed by a tensile overload peak of equal magnitude produced the maximum reduction in crack opening stress for physically short cracks in fatigue specimens. For simplicity, this load sequence is referred to as a "fully reversed overload" [3]. Overloads of yield-magnitude tend to decrease the crack opening stress levels and increase the effective stress range. Lower crack opening stress levels tend to make cycles following the overload more effective in causing damage, even at levels of stress that would not normally cause damage in the component. Overloads of lesser magnitudes may affect damage in a different manner.

Many components are also subject to corrosion while subjected to a variable amplitude load spectrum. This phenomenon, termed corrosion-fatigue (CF), has an especially detrimental effect on the longevity of structures and will lead to the premature failure of a component in service. An example of such a component is the wing spar of an aircraft that is flown regularly at altitudes close to the surface of the ocean. The primary mechanism that shortens the life of a susceptible material in corrosion-fatigue is premature crack initiation as a result of the formation of corrosion pits on the surface of the material. These pits quickly evolve into cracks, which, through the combined action of fatigue and further corrosion will progress to the point of failure of the component and possibly the entire structure.

This investigation reports the results of corrosion-fatigue experiments conducted on 7075-T651 aluminum alloy subjected to periodic reversed overloads in air and in a simulated seawater environment. The periodic overload spectrum has been shown to give fatigue data that are reliable and can be used to obtain accurate to slightly conservative fatigue life predictions for metal structures subjected to variable amplitude loading in air [1–4]. Constant amplitude tests carried out in lab-air and simulated seawater environment are also presented for purposes of comparison.

2. Experimental program

2.1. Materials

7075-T651 aluminum alloy is a high strength aluminum that is used primarily in aerospace structural components such as in the Canadian Air Force CP-140 Aurora maritime patrol aircraft and the CC-130 Hercules transport aircraft. The typical chemical composition and the mechanical properties of this alloy are given in Table 1.

All aluminum specimens, with the geometry and dimensions as shown in Fig. 1, were machined from extruded rods of the material. The loading axis of each specimen was parallel to the direction of the elongated grains. The specimens were machined on a computer numerically controlled (CNC) lathe using progressively shallower cuts on the gage section to minimize the residual stresses near the surface of the specimen.

The specimens were polished parallel to the loading axis with progressively finer grades of sandpaper starting at 320-grit to 400-grit, and finishing with 600-grit emery cloth. This procedure was used to remove machining marks perpendicular to the load axis that would cause stress concentrators in the area. The gage section was examined using a light microscope with 30× magnification to ensure that all the machine marks were removed. Isopropyl alcohol was used to clean the surface of any grease or oil. Finally, the specimen was wiped using soft paper towel in the direction of loading to remove any debris remaining from the polishing process.

3. Testing environments and load spectra

Two different testing environments were used in this investigation: a lab-air environment, and a simulated seawater environment (3.5 wt% NaCl in de-ionized water). Details of the testing environments are detailed in Table 2.

Table 1
Properties of 7075-T651 aluminum alloy

Zn	Mg	Cu	Cr	Mn	Ti	Fe	Si	Al
a. Nominal chemical composition (wt%) [47]								
5.1–6.1	2.1–2.9	1.2–2.0	0.18–0.28	0.3	0.2	0.5	0.4	Remainder

0.2% Offset yield strength	Ultimate tensile strength	Modulus of elasticity	Elongation
b. Mechanical properties in L-direction [47]			
469 MPa	538 MPa	72,000 MPa	7%

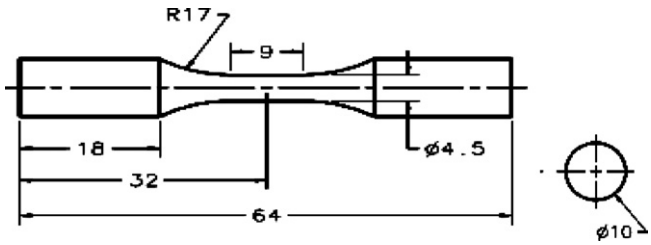

Fig. 1. Dimensions (mm) of 7075-T651 fatigue coupons.

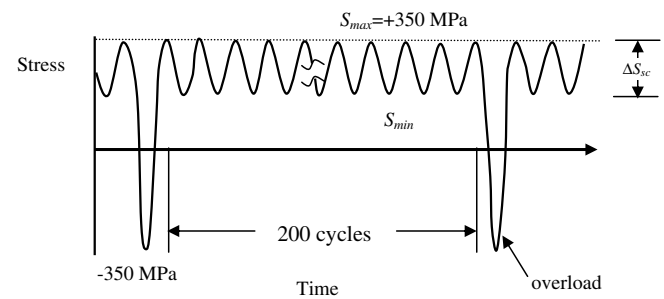

Fig. 2. Periodic overload loading spectrum for 7075-T651 aluminum alloy.

3.1. Lab-air

The data for the tests in lab-air were obtained from previous investigations by DuQuesnay and Lynn [1,6]. These previous investigations consisted of periodic reversed overload and constant amplitude tests performed on 7075-T651 aluminum alloy using coupons with the dimensions presented in Fig. 1. These lab-air tests were performed at frequencies ranging from 15 to 25 Hz. The overload spectra used were identical to those used in simulated seawater tests in the present study.

For this study, several additional constant amplitude (CA) tests were performed in the lab-air environment to validate the values obtained in the previous investigations. These tests were performed in stress-control at frequencies ranging from 10 to 25 Hz on a closed-loop servo-controlled electro-hydraulic testing system. The humidity was not formally monitored but the average humidity level during testing was 55% ± 10%. The tests used a constant amplitude sinusoidal waveform at stress ranges, ΔS, ranging from 400 MPa (±200 MPa) to 800 MPa (±400 MPa).

Fatigue tests were also carried out using a periodic reversed overload spectrum in the two environmental conditions. This loading spectrum consisted of a periodic, fully-reversed overload of near-yield magnitude (±350 MPa) followed by 200 smaller cycles (ΔS_{sc}) at a high stress ratio as seen in Fig. 2. The stress range of the smaller cycles was varied between tests by changing the minimum stress of the smaller cycles, S_{min}, while maintaining the maximum stress, S_{max}, at the overload magnitude.

3.2. Simulated seawater

The periodic overload tests on specimens carried out in a seawater environment were performed in load-control on a closed-loop servo-controlled electro-hydraulic testing system (Fig. 3). The gage sections of the aluminum specimens were enclosed in a large plastic corrosion cell which held approximately 180 cm^3 of simulated seawater maintained at a steady-state temperature of 33 °C ± 1 °C. The solution was aerated with lab-air in the reservoir and then circulated through the corrosion chamber at a rate of 15 cm^3/s. A fresh reservoir was prepared for each test. Each reservoir contained a litre of simulated seawater solution made from laboratory grade sodium chloride and de-ionized water to form a 3.5 wt% NaCl solution with an initial pH of 7.

The corrosion-fatigue tests were performed in load-control at a nominal frequency of 5 Hz. This frequency was selected to provide significant exposure time while still allowing the tests to be completed in a timely manner. This is a common frequency chosen in corrosion-fatigue tests in other investigations [5,8–10]. A few additional tests were performed at lower frequencies (0.02, 0.1 Hz) to determine the effect of exposure time on the corrosion-fatigue behaviour of the alloy. In one test, the aluminum coupon was pre-exposed for 30 h (the average length of the longer-duration tests) to ascertain the effects of pre-exposure on crack initiation and corrosion-fatigue life. All coupons were subjected to 5 min of pre-exposure in the corrosion chamber before the start of fatigue testing to ensure steady-state conditions for all the coupons tested. Constant amplitude corrosion-fatigue results were taken from the SAE Handbook [7] and are presented for comparison purposes.

4. Results and discussion

4.1. Plotted results

The results of fatigue testing of 7075-T651 aluminum alloy with periodic overloads in lab-air as well as simulated seawater are given in Fig. 4 as a function of the stress range of the small cycles, ΔS_{sc}, and the total number of cycles to failure, N_f. For comparison, the results have been plotted in conjunction with those for constant amplitude fully reversed loading ($R = -1$) in air, constant amplitude fully reversed loading ($R = -1$) in simulated seawater [11], and periodic reversed overloads in air.

Table 2
Testing environments

Environment	Humidity	Average temperature	Specimens	Spectrum	Corrosion/Chamber
Lab-air	Not monitored	23 °C ± 1 °C	Al	Constant amp./Periodic overload	N/A
Seawater (large)	Fully immersed	33 °C ± 1 °C	Al	Constant amp./Periodic overload	3.5 wt% NaCl solution/large chamber

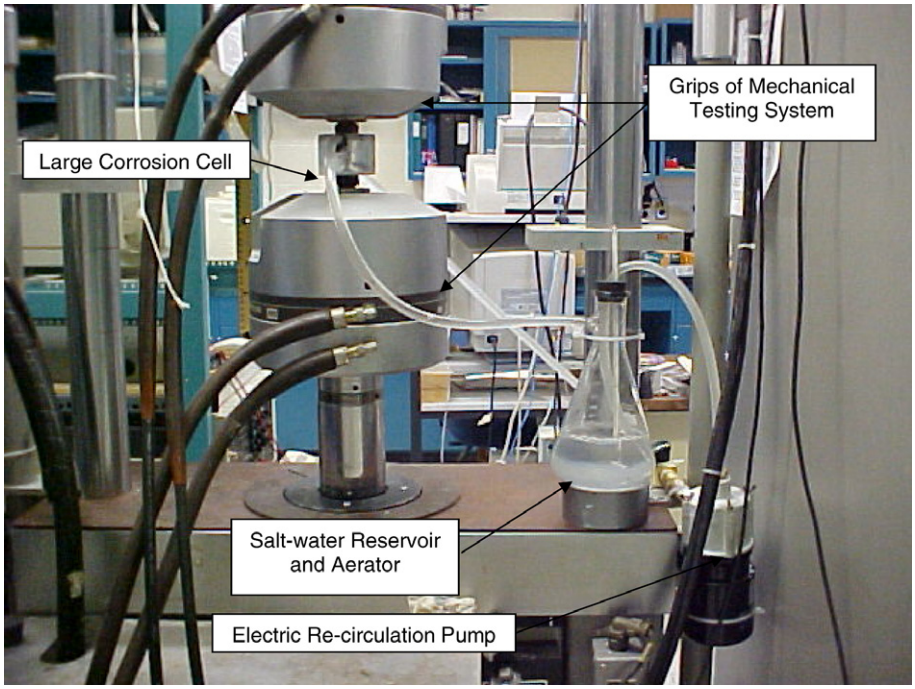

Fig. 3. Corrosion-fatigue apparatus used in 'large-coupon testing' showing the mechanical testing system, the large corrosion chamber, the salt-water reservoir/aerator, and the electric recirculation pump.

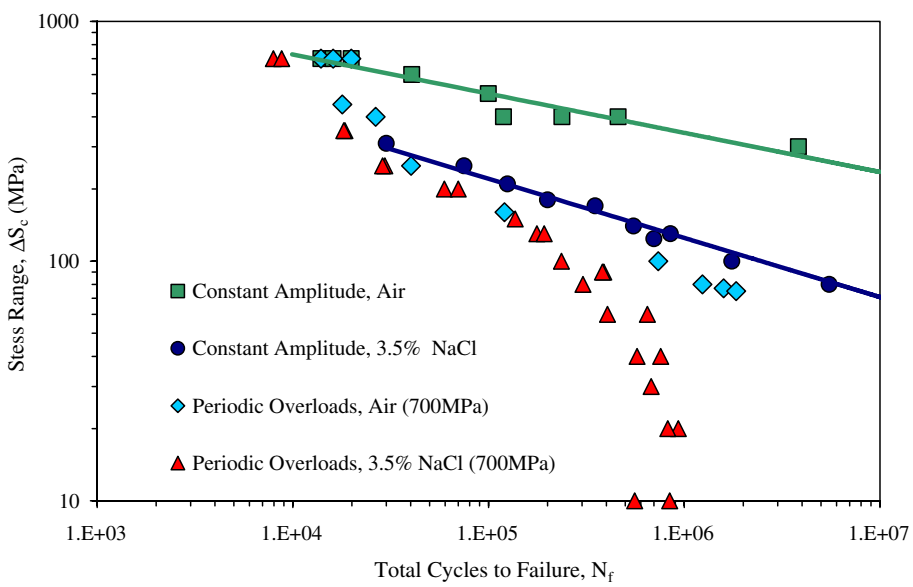

Fig. 4. Fatigue life data for 7075-T651 aluminum alloy in air, and simulated seawater.

There is a significant reduction in the fatigue strength and the fatigue life of the specimens subject to the constant amplitude corrosion-fatigue as well as those subject to combined corrosion-fatigue and overloads. At stress levels below $\Delta S_{sc} = 100$ MPa, there is a reduction in the corrosion-fatigue life of about a factor of three when compared to the lab-air overload data. The stress-life data of specimens subjected to corrosion-fatigue with overloads does not differ substantially from the lab-air overload data in the "middle region" from $\Delta S_{sc} = 350$ MPa to 120 MPa; however, the data diverges noticeably at stresses below $\Delta S_{sc} = 100$ MPa. The lab-air overload data follows a horizontal asymptote to an endurance-limit of $\Delta S = 75$ MPa [3], while the corrosion-fatigue overload data approaches a life-limit of roughly 9100 cycles. Through extrapolation, one can find an endurance-limit of $\Delta S = 130$ MPa, corresponding to 5×10^8 cycles is reached for the lab-air constant amplitude loading. Conversely, an endurance-limit of approximately 25 MPa is attained through extrapolation in the constant amplitude spectrum cycled in simulated

seawater (at a life 5×10^8 cycles). The endurance-limit region was not well tested due to the lack of specimens.

In order to understand the effects of periodic overloads on the corrosion-fatigue behaviour, it is convenient to first remove the damage done by the overloads and to examine the equivalent life of the small cycles, as described in the following section.

4.2. Analysis of equivalent life

Both tensile overloads and compressive overloads of yield-magnitude or greater tend to decrease the crack opening stress level and increase the damage caused by the subsequent smaller cycles [1–3,12]. It has been demonstrated that the damage accumulation rates increase following an overload of near-yield magnitude and stay elevated for a number of cycles thereafter. The explanation for this phenomenon derives from the reduction of the crack opening stress level following a yield-magnitude overload. Large compressive overloads tend to flatten asperities and flatten material in the crack wake, while tensile overloads of this magnitude cause large scale yielding in front of the crack and leave the crack open upon unloading [2]. Consequently, compression-tension (CT) overloads of near-yield magnitude tend to cause the largest drop in crack opening stress with subsequent cycles causing the most damage when compared to other types of overloads of yield-magnitude such as compression (C), tension (T), and tension-compression (TC). The damage accumulation rates tend to stay constant for a number of cycles following the overload depending on the material in question. For example, – the damage accumulation rates in 2024-T351 aluminum alloy stays constant for approximately 250 cycles before commencing a slow logarithmic decay to steady state levels.

It is often of interest to separate the damage done by the small cycles in a variable amplitude load history from the damage done by periodic overloads. The damage done by the small cycles is characterized by the equivalent number of small cycles to failure N_{eq}, calculated by removing the damage done by the overload cycles according to Miner's rule:

$$N_{eq} = \frac{N_{sc}}{1 - \frac{N_{ol}}{N_{fo}}} \tag{1}$$

where N_{ol} is the number of overloads and N_{sc} is the number of small cycles applied to failure ($N_f = N_{sc} + N_{ol}$, where N_f is the total number of cycles to failure), and N_{fo} is the number of overload cycles alone required to cause failure. The calculated value of N_{eq} gives an estimate of the small cycle fatigue damage in a component that is subject to a load history that consists of both small cycles and periodic overloads. This methodology of equating equivalent life is documented in detail by DuQuesnay [3].

The equivalent life of the aluminum specimens subject to small cycles in both the corrosion-fatigue and lab-air overload tests were calculated using Eq. (1) and plotted in Fig. 5. The effect of the periodic overloads in the load spectra was removed using this calculation, providing the effective fatigue lives of only the small cycles. The value of N_{fo} (number of overloads alone to cause failure) was calculated from the average life of two overload tests for the corrosion-fatigue experiments and the average life of three overload tests in air. The magnitudes were $N_{fo} = 8361$ cycles in 3.5 wt% NaCl and $N_{fo} = 16{,}625$ cycles in lab-air. The mathematical exclusion of overloads caused an increase in fatigue life of about a factor of two at stress levels below 100 MPa. The equivalent stress-life data for the lab-air fatigue tests and the corrosion-fatigue were very close, with the overlap of some data in the "middle-region" between stress levels of 350 MPa and 120 MPa. This middle region mirrors the same region in Fig. 4 with little difference in the fatigue life of specimens cycled in lab-air or corrosion, even with the removal of overload damage.

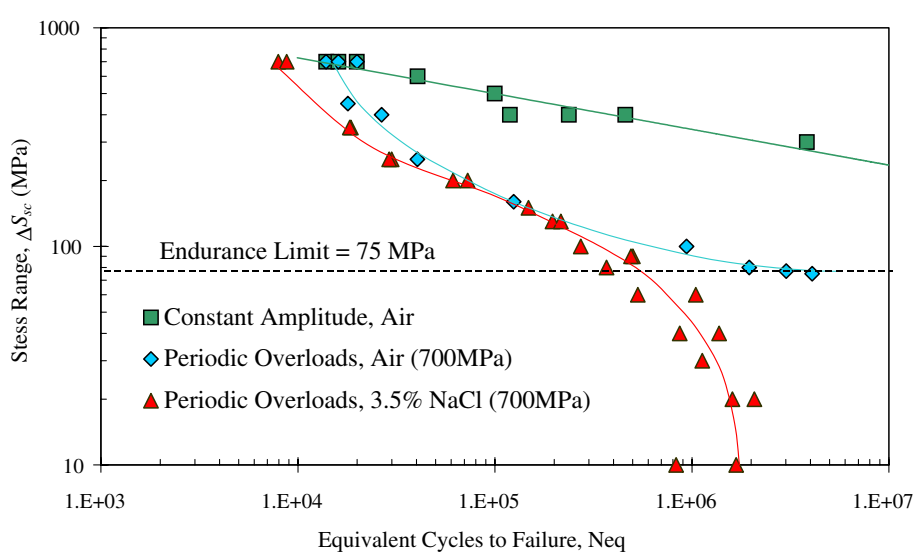

Fig. 5. Equivalent fatigue life data for 7075-T651 aluminum alloy in air and simulated seawater.

The data diverged in a similar manner as in Fig. 4 at $\Delta S_{sc} = 100$ MPa. Below this point, there was a significant effect of overloads on the small cycle fatigue life of the aluminum in salt-water. While the air-overload data approached an endurance-limit of 75 MPa at almost 9100 cycles, the small cycle air-overload data reached the endurance-limit at close to four and a half million cycles. The small cycle corrosion-fatigue-overload data continued to a life-limit at approximately two million cycles at $\Delta S_{sc} = 20$ MPa. It can be seen that the endurance-limit of the material was eliminated for specimens cycled in corrosion-fatigue.

The equivalent life of the specimens was comparable to the corrosion data without overloads above $\Delta S_{sc} = 200$ MPa, but was reduced below this level. At $\Delta S_{sc} = 130$ MPa, the equivalent-life data was already out by a factor of four from the data in Fig. 4. At $\Delta S_{sc} = 90$ MPa, the data diverged by about a factor of ten. There is an interaction between periodic overloads and corrosion-fatigue as the specimens are cycled closer and closer to the constant amplitude CF endurance-limit. This interaction can be explained by strain-assisted dissolution, which accelerates pitting and dissolution at the crack tip due to strains caused by high stress [5,14,15].

5. Fracture surfaces

Examination of the surfaces of the corrosion-fatigue specimens showed that crack initiation was typically from stress concentrations caused by pits forming on the surface of the specimen. Other studies have found that pits were the initiators of cracks as well [5,9,16–21]. Multiple pit sites could be found on coupons in all but the highest stress levels (i.e., $\Delta S = 700$ MPa and $\Delta S_{sc} = 350$ MPa), and in most cases cracks would initiate from several sites where pits could be found on the surface of the specimen. Cracks that propagated from multiple pitting sites would often meet, forming a large crack front that would inevitably lead to the failure of the specimen. This can be seen in the coupon subjected to periodic overloads in simulated seawater at $\Delta S_{sc} = 80$ MPa in Fig. 6. It is believed that these pits formed at the site of inclusions (such as particles of $Al_{23}CuFe_4$, and Al_2CuMg.) These inclusions are typical in heterogeneous alloys such as 7075-T651 [18,22].

At higher stress levels, there was evidence of anodic slip dissolution as seen in the flat morphology at crack initiation sites of coupons cycled at $\Delta S = 700$ MPa and $\Delta S_{sc} = 350$ MPa. Examination of the fracture surfaces, such as that seen in Fig. 7, found that there was no pit at the crack initiation site and that the area immediately around the site was almost featureless. It is postulated that slip-induced anodic dissolution was responsible for the initiation of the crack in this area. This is caused by a large stress acting as a driving force, which produces slip steps in the material that propagate the crack [14]. Anodic slip dissolution appears to be the dominant mechanism for crack propagation in these high stress regions, while pitting was the cause of crack propagation in specimens subject to lower cyclic stress levels [14].

The surface morphology of corroded specimens differed substantially from specimens tested in lab-air. The surface showed smooth and distinct river lines, which led to the

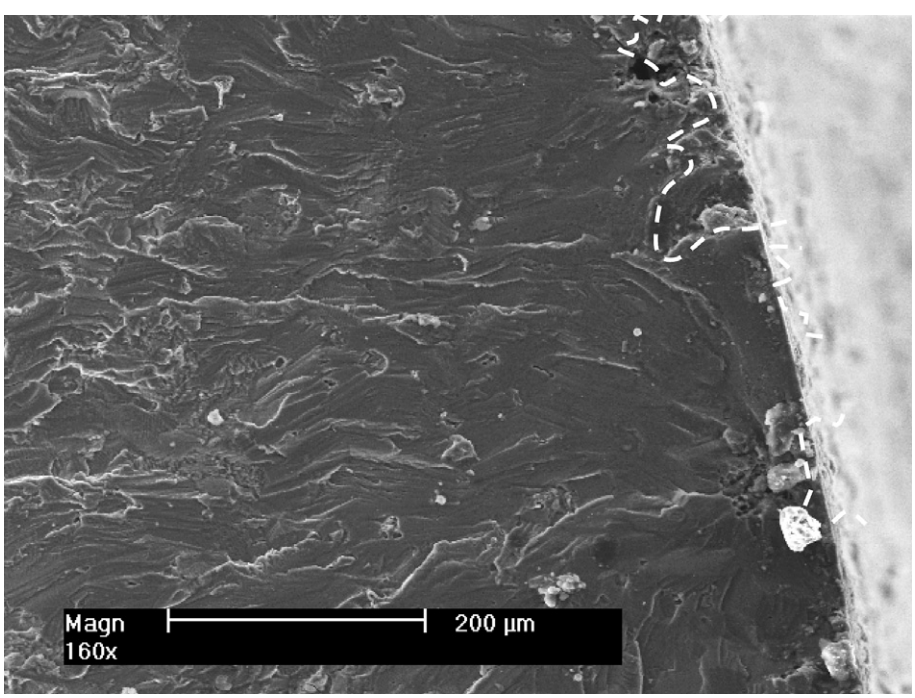

Fig. 6. Multi-scale pitting can be seen at the fracture initiation point outlined in white. The pits vary in size with average lengths between 25 µm and 105 µm. (Specimen cycled in NaCl solution, $\Delta S_{sc} = 80$ MPa, $N_f = 303588$ cycles.)

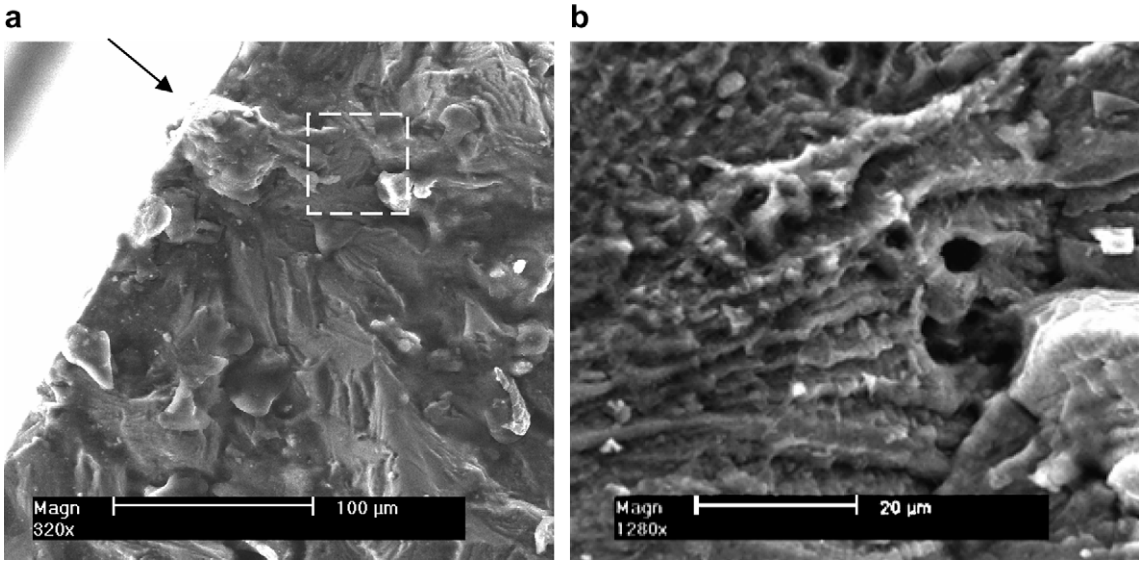

Fig. 7. Magnification of fracture surfaces. (Specimen cycled in NaCl solution, $\Delta S = 700$ MPa, $N_f = 8769$ cycles.) (a) A magnification of the fracture initiation site. An arrow indicates the initiation point. (b) A close-up of the striations near the fracture initiation site.

crack initiation site. This is typical of what is observed when cycling 7XXX series aluminum alloys in air and are a result of extensive plastic blunting by shear at the crack-tip [14,18]. In Fig. 7b, the striations of a coupon cycled in corrosion-fatigue at $\Delta S = 700$ MPa are rough and jagged. These "brittle striations" are typically observed in cycling in aqueous chloride solutions for Al–Zn–Mg aluminum alloys and provide evidence of an embrittlement phenomenon [14,18,23].

5.1. Corrosion-fatigue in constant amplitude

The reduction in fatigue life due to corrosion was especially evident in the constant amplitude corrosion data which displayed a distinct decrease in life compared to the constant amplitude cycling in lab-air. For example, at $\Delta S = 450$ MPa the fatigue life was reduced by a factor of 40 (i.e. 8000 cycles in simulated seawater as compared to 300,000 cycles in lab-air). The reduction in fatigue life is primarily a result of premature crack initiation caused by pitting. It is postulated that anodic slip dissolution would have a greater effect on fatigue life at higher stress levels, with pitting having a greater effect at lower stress levels [14]. At higher stress levels, corrosion pits did not have enough time to form and initiate a crack. At these high stress levels, the cyclic loading provided enough mechanical driving force to form slip steps that acted as stress concentrators. Significant reductions in the fatigue life of 7XXX series aluminum alloys under similar tests were reported in the literature [14,18]. This reduction in fatigue life is also supported by fractographic evidence. At high stress-levels, a pit was not found at the crack initiation point and displayed a flat and featureless morphology near the crack initiation site. This morphology is characteristic of crack initiation and propagation through anodic slip dissolution [14,18].

5.2. Corrosion-fatigue and periodic overloads

The specimens subject to corrosion-fatigue had slightly shorter fatigue lives at higher stress-levels, but never larger than a factor of two. In the "middle region", between $\Delta S_{sc} = 350$ MPa and $\Delta S_{sc} = 120$ MPa, the fatigue data almost overlap. Corrosion-fatigue did not seem to be a factor at stress levels above 120 MPa when periodic overloads were applied. This differs considerably from what happened in corrosion-fatigue when there were no overloads present. In this middle region, the overloads were dominant in causing the reduction in fatigue life. Periodic overloads caused the crack tip to stay open at a lower crack-opening stress level, which allowed a larger effective stress range to produce damage in the material. It is believed that at stress levels above 100 MPa, anodic slip dissolution was the dominant mechanism that started and propagated the cracks. This is supported by fractographic evidence such as in Fig. 7, where no pit was seen near the crack initiation point at $\Delta S = 700$ MPa and $\Delta S_{sc} = 350$ MPa. It is proposed that periodic overloads created the mechanical driving force required to cause slip steps that provided stress concentrations large enough to start and propagate a crack at stress levels of $\Delta S_{sc} = 100$ MPa and above.

At $\Delta S_{sc} = 100$ MPa and below, the corrosive environment had a significant effect on the fatigue life. While the air-overload data approached an endurance-limit of 75 MPa, the corrosion-fatigue-overload data continued to a life-limit of approximately one million cycles at $\Delta S_{sc} = 20$ MPa. The elimination of an endurance-limit in specimens cycled in corrosion-fatigue was due to a combination of effects. Crack initiation at such low levels of stress would have occurred primarily by the stress concentration caused by the pits that formed due to the aggressive action of the salt-solution. Corrosion pits as small as 60 µm can transition into a long crack [5,20].

It is hypothesized that periodic overloads provided the mechanical driving force that was required to start a crack once a pit was large enough to cause a significant stress concentration. Furthermore, the overload caused a drop in the crack opening stress and allowed the normally innocuous small cycles to cause damage. It is suspected that hydrogen embrittlement [5,21], and acidification inside the pit [22] made the area at the bottom of the pit brittle and more susceptible to cracking. This is supported by the fractographic results which revealed that cracks typically grew from pits on the surface of the specimen at $\Delta S_{sc} = 20$ MPa and 80 MPa. These figures also revealed cracking of the fracture surface, which was most probably caused by the combination of embrittlement and the large stresses produced by periodic overloads. Conversely, an endurance-limit was still evident when cycled in lab-air. At stress levels below $\Delta S_{sc} = 75$ MPa, a smooth straight specimen requires a stress concentration (such as a pit in corrosion-fatigue) to overcome microstructural barriers and allow the formation and propagation of a crack.

5.3. Stress corrosion cracking

Stress corrosion cracking (SCC) can incur in ductile metals under the combined application of a tensile stress and specific corrosive environments. 7075-T6 aluminum alloy is known to be susceptible to SCC when exposed to a chloride solution. Stress corrosion can result in premature cracking of a component without cycling or at cyclic stress levels well below those normally required to initiate mechanical cracks. Stress corrosion cracking in aluminum alloys is characteristically intergranular and is often characterized by spider-web like cracks between the grain boundaries on the surface [24]. Given that there was a high tensile mean stress applied to the specimens, they were examined for indications of SCC after testing. Examination of the fracture surfaces clearly show that the cracks were intragranular precluding SCC as the primary failure mechanism. It is postulated that the relatively short exposures of the specimens to the corrosive environment during testing was insufficient to allow stress corrosion cracks to propagate. The transgranular fracture features suggest a corrosion-fatigue (CF) mechanism was predominant in the experiments performed. However, it must be acknowledged that at more prolonged exposures SCC might impact on the fatigue life of the specimens.

5.4. Other effects

Several aluminum specimens were cycled under constant amplitude loading ($\Delta S = 700$ MPa) in corrosion-fatigue at 0.02 Hz and 0.1 Hz to determine the effect of loading frequency on fatigue life. These specimens displayed slightly reduced fatigue-lives when compared with the specimens cycled at 5 Hz. The difference in fatigue life was small except at extremely low frequencies; for example at 5 Hz the average fatigue life was 8361 cycles; at 0.1 Hz the average fatigue life was 5073 cycles; and the fatigue life at 0.02 Hz was 3191 cycles. Gordon et al. [25] found little difference in fatigue life for frequencies between 0.1 Hz and 5 Hz for a 7075-T7651 aluminum alloy. It is hypothesized that the reduction in fatigue life in the coupon cycled at 0.02 Hz was from a number of effects: increased residency time in the corrosive solution (allowing larger pits to be formed) and hydrogen embrittlement. At 0.02 Hz, the test lasted approximately 44 h, which was similar to the test length of the coupon cycled at $\Delta S_{sc} = 20$ MPa (45 h). This allowed larger pits to form and ensured large enough stress concentrations for a crack to form. The hydrogen embrittlement mechanism also had more time to make the tip of the crack brittle further facilitating the propagation of the crack.

One coupon was subjected to 30 h of pre-corrosion before cycling at constant amplitude in corrosion-fatigue at $\Delta S = 700$ MPa. This specimen broke at 5124 cycles which is slightly lower than the other corrosion-fatigue specimens tested in this study. The pre-corrosion gave time for pits to form on the surface of the material, thus producing a stress concentration that led to premature crack initiation [14,22,25,26]. Hence, premature crack initiation from pits on the surface formed during pre-corrosion caused the decrease in fatigue life.

The results suggest that the approach taken by many researchers to pre-corrode coupons prior to performing spectrum fatigue testing gives similar fatigue results as for simultaneous corrosion and fatigue; the former is much easier to achieve in the laboratory.

Exposure time would have a significant effect in structures used in-service that are subject to both corrosion-fatigue and a variable-amplitude loading spectrum. In the Canadian Forces, some maritime aircraft (e.g., Sea King, and Aurora) have been in service for over thirty years. This means that the structure of the aircraft would be at risk of failure if proper corrosion-control procedures were not in place. Several types of corrosion (including exfoliation, pitting, and stress corrosion cracking) can be found in aircraft applications and pitting is but one form. A residency time of a few hours in seawater can cause pitting that decreases the fatigue life of a component. If pitting is not removed in a timely manner, as can happen in some non-inspectable areas, it could cause premature crack initiation in aircraft components. It has been shown in other studies that corrosion-fatigue at frequencies above 20 Hz (which are typical flight loading frequencies), would not be as damaging to the material as corrosion-fatigue below this frequency for a given stress level [21,27].

6. Conclusions

The effects of overloads on the corrosion-fatigue of 7075-T651 aluminum alloy have been presented. The material was subjected to near-yield magnitude overloads in air and in a 3.5 wt% NaCl simulated seawater solution.

Several conclusions can be drawn from the results and discussion presented:

The fatigue life of 7075-T651 aluminum alloy is reduced significantly by the application of periodic overloads in 3.5 wt% NaCl when compared to equivalent tests performed in lab-air and without overloads.

The endurance-limit of 7075-T651 aluminum alloy was eliminated by the combination of overloads and the simulated seawater environment.

Corrosion-fatigue did not have a large effect on the fatigue life of 7075-T651 aluminum alloy cycled with periodic overloads in the region between $\Delta S_{sc} = 450$ MPa and $\Delta S_{sc} = 100$ MPa. In this region, the fatigue life of corrosion-fatigue specimens was equivalent to specimens cycled in lab-air.

Below $\Delta S_{sc} = 100$ MPa, there was a distinct reduction in the fatigue life of all specimens cycled with periodic overloads in corrosion-fatigue when compared to those cycled in air. It is concluded from fractographic evidence that this reduction in life was due to premature crack initiation from corrosion pits formed on the surface of the specimen.

Acknowledgement

This research was supported by the Department of National Defence (DND), Canada

References

[1] DuQuesnay DL. Measuring the fatigue resistance of aluminum alloys under spectrum loading. In: Proceedings of the Canadian forces ASIP symposium, Ottawa, ON; 1994.

[2] Topper TH, DuQuesnay DL. The effects of overloads in service load histories on crack closure and fatigue damage. Society of automotive engineers, Paper # 2001-01-4079, Warrendale, PA; 2001.

[3] DuQuesnay DL. Applications of overload data to fatigue analysis and testing. In: Braun AA, McKeighan PC, Nicolson AM, Lohr RD, editors. Applications of automation technology in fatigue and fracture testing and analysis. ASTM 1411, vol. 4. West Conshohocken, PA: American Society for Testing and Materials; 2002.

[4] Khalil M, DuQuesnay D, Topper TH. Prediction of crack opening stress levels for service loading spectra. In: Braun AA, McKeighan PC, Nicolson AM, Lohr RD, editors. Applications of automation technology in fatigue and fracture testing and analysis. ASTM STP 1411. West Conshohocken, PA: American Society for Testing and Materials; 2002.

[5] Murtaza G, Akid R. Corrosion fatigue short crack growth behaviour in a high strength steel. J Int Fatigue 1996;18(8):557–66.

[6] DuQuesnay DL, Lynn AK. Computer simulation of variable fatigue crack initiation behaviour using a new strain-based cumulative damage model. Int J Fatigue 2002;24:977–86.

[7] Rice RC, editor. SAE fatigue design handbook. Warrendale, PA: SAE International; 1997.

[8] Chen GS, Wan K-C, Gao M, Wei RP, Flournoy TH. Transition from pitting to fatigue crack growth – modeling of corrosion fatigue crack nucleation in a 2024-T3 Aluminum alloy. Mater Sci Eng 1996;A219:126–32.

[9] Murtaza G, Akid R. Empirical corrosion fatigue life models of a high strength steel. Eng Fract Mech 2000;67(5):461–74.

[10] Pao PS, Imam MA, Cooley LA, Yoder GA. Comparison of corrosion-fatigue cracking of Al-Li alloy AA 2090-T8E41 and alloy AA 7075-T651 in salt water. Corrosion 1989;45(7):530–5.

[11] Rice RC, editor. SAE fatigue design handbook. Warrendale, PA: SAE International; 1997.

[12] Nolting AE and DuQuesnay DL. The effect of mean stress and strain on fatigue damage following overloads. Society of automotive engineers, 2003-01-0910.

[13] DuQuesnay DL, Topper TH, Yu MT, Pompetzki MA. The effective stress range as a mean stress parameter. Int J Fatigue 1992;14(1):45–50.

[14] Lin C-K, Yang S-T. Corrosion fatigue behaviour of 7050 aluminum alloys in different tempers. Eng Fract Mech 1998;59(6):779–95.

[15] Murtaza G, Akid R. Empirical corrosion fatigue life models of a high strength steel. Eng Fract Mech 2000;67(5):461–74.

[16] Shi P, Mahadevan S. Damage tolerance approach for probabilistic pitting corrosion fatigue life prediction. Eng Fract Mech 2001;68:1493–507.

[17] Rokhlin SI, Kim J-Y, Nagy H, Zoofan B. Effect of pitting corrosion on fatigue crack initiation and fatigue life. Eng Fract Mech 1999;62:425–44.

[18] Duquette DJ, Corsetti LV. The effect of mean stress and environment on corrosion fatigue behaviour of 7075-T6 aluminum. Metall Trans 1974;5(May):1087–93.

[19] Wan K-C, Chen GS, Gao M, Wei RP. Interactions between mechanical and environmental variables for short fatigue cracks in a 2024-T3 aluminum alloy in 0.5 M NaCl solutions. Metall Mater Trans A 2000;31A(March):1025–34.

[20] Jabubowski M. Fatigue crack propagation in austenitic stainless steel under low frequency loading and salt water conditions. Fatigue Fract Eng Mater Struct 1998;21:937–46.

[21] Hasse I, Nocke K, Worche H, Zouhar G, Tempus G. An investigation of the fatigue behaviour of aluminum alloy AA 6013 T6 in a corrosive medium. Prakt Metallogr 2001;36(3).

[22] Wei RP. Material aging and reliability of engineered systems. In: Kane RD, editor. Environmentally assisted cracking: predictive methods for risk assessment and evaluation of materials. Equipment and structures, ASTM STP 1401. West Conshohocken, PA: American Society of Testing and Materials; 2000. p. 3–19.

[23] Du ML, Chaing FP, Kagwade SV, Clayton CR. Influence of Corrosion on the Fatigue Properties of Al 7075-T6. J Test Eval, JTEVA 1998;26(3):260–8.

[24] Arsenault, Ghali E. Prevention of environmentally assisted cracking of structural aluminum alloys by Al and Al-5Mg thermal sprayed coatings using different surface preparation techniques. In: Conference of metallurgists (Com 2006) aerospace materials and manufacturing: Symposium Proceeding, Montreal, Quebec, Canada; 1–4 October, 2006. p. 61.

[25] Gordon DE, Manning SD, Wei RP. Effects of salt water environment and loading frequency on crack initiation in 7075-T7651 aluminum alloy and Ti-6Al-4V. In: Proceedings of corrosion cracking program and related papers presented at International Conference and exposition on fatigue corrosion cracking. Fracture mechanics and failure analysis. Metals Park, OH, USA: ASM; 1986. p. 157–65.

[26] Gough HJ. Corrosion-fatigue of metals. J Inst Met 1932;49:17–92.

[27] Bannantine JA, Comer JJ, Handrock JL. Fundamentals of metal fatigue analysis. Toronto: Prentice-Hall Inc.; 1990.